

Articles

Contribution from the Department of Chemistry,
Northern Illinois University, DeKalb, Illinois 60115

MCD Spectra for the Mercury $^1S_0(6s^2) \rightarrow ^3P_1(6s6p)$ Atomic Resonance Transition in the Vapor Phase and in Solution

W. Roy Mason

Received July 16, 1987

Absorption and magnetic circular dichroism (MCD) spectra at room temperature are reported for Hg vapor in air and for saturated solutions of Hg in cyclohexane, acetonitrile, and water in the region of the $^1S_0 \rightarrow ^3P_1$ atomic resonance transition at 253.65 nm. The vapor-phase spectrum consists of a narrow absorption line and a symmetric positive A term at 0.1–0.5 T but resolves into two Zeeman absorption components and two B terms of opposite sign at 7 T. Evaluation of \bar{A}_1/\bar{D}_0 from a moment analysis of 0.1–0.5-T spectra gives a value of $+2.88 \pm 0.19$, which is interpreted in terms of spin-orbit coupling of the 3P_1 and 1P_1 states of the $6s6p$ excited configuration. The solution spectra show broad unsymmetrical positive A terms for the MCD of all three solvents and broad absorption with evidence of band splitting for cyclohexane and acetonitrile (absorption band(s) for water is (are) too weak to measure). \bar{A}_1/\bar{D}_0 for cyclohexane solution gives a value of $+2.7 \pm 0.1$. The lack of change in \bar{A}_1/\bar{D}_0 from vapor to solution and the origin of the splitting of the broad solution spectra are discussed in terms of Hg-solvent interaction and excited-state (Jahn-Teller) distortion.

Introduction

The lowest energy electronic excitation for metal ions of $6s^2$ electron configuration gives rise to the $^1S_0(6s^2) \rightarrow ^3P_1(6s6p)$ transition, which although formally spin-forbidden may be quite intense because of the breakdown of spin selection rules by strong spin-orbit coupling of the 3P_1 state with the higher energy $^1P_1(6s6p)$ state.¹ This transition is believed to be the origin of the intense UV bands and strong magnetic circular dichroism (MCD) A terms for Tl(I), Pb(II), and Bi(III) in aqueous acid solution studied recently in this laboratory.² An extension of this study to isoelectronic Hg(0) was at first considered impractical due to the absence of complex formation to give a suitable solution species. However, on learning of the measurable solubility of metallic Hg in water³ and nonaqueous solvents,⁴ we reconsidered the study of Hg(0) in solution because the $^1S_0 \rightarrow ^3P_1$ atomic resonance transition at 253.652 nm is known in the gas phase to be intense and to exhibit Zeeman splitting in a magnetic field⁵—features that should make it possible to observe this transition in solution by MCD spectroscopy. The absorption spectra of Hg(0) in aqueous and nonaqueous solutions in the region of the $^1S_0 \rightarrow ^3P_1$ transition are broad and show evidence of splitting into two or more components.⁴ The nature of the dissolved species is not entirely clear but on the basis of Beer's law studies, atomic Hg rather than Hg_n clusters was suggested.⁴ Further, matrix-isolated Hg in solid N_2 or solid noble gas matrices shows a remarkably similar absorption broadening and band splitting,⁶ and MCD spectra of Hg in N_2 or Ar matrices revealed a complicated unsymmetrical A term in the $^1S_0 \rightarrow ^3P_1$ energy region.⁷ The origin of the complex spectra for Hg in solution and in solid matrices is not understood and provided motivation for the present study. This report is concerned with room-temperature MCD and absorption spectra in the region of the $^1S_0 \rightarrow ^3P_1$ transition for Hg in cyclohexane solution and, for comparison purposes, for Hg in the vapor phase. Some qualitative spectra for Hg in acetonitrile

or water are also presented, but in these cases low signal levels and unfavorable signal to noise ratios made precision measurements difficult.

Experimental Section

Solutions of Hg in cyclohexane were prepared by shaking triply distilled Hg metal with spectroquality solvent over a period of several days at room temperature. Saturated solutions resulted within a few hours, but the solutions were allowed to settle undisturbed for at least 24 h before use. The Hg concentration was determined by Hg-vapor atomic absorption⁸ to be $(5.0 \pm 0.5) \times 10^{-7}$ M. Saturated solutions of Hg in acetonitrile or water were prepared in a similar way but were not analyzed for Hg content because the quality of the spectra did not justify quantitative precision. Absorption and MCD spectra were determined simultaneously and synchronously along the same light path by means of a computer-controlled spectrometer described earlier.⁹ Magnetic fields to 7 T were obtained by a superconducting magnet system (Oxford Instruments SM2-7, fitted with a room-temperature bore tube). The magnetic field homogeneity was better than 1% for measurements using cells of path lengths of 2 cm or less, but for longer path lengths a correction had to be applied due to field inhomogeneity at distances > 2 cm from the bore center. This correction amounted to a 12% reduction in the average field over the sample volume when 10.0-cm-path cells were used. The solution measurements were made by using 10.0-cm quartz cells and were corrected for solvent blank. Beer's law was found to hold for a 10-fold dilution of the saturated cyclohexane solution. Spectral resolution for the solution measurements where the spectra are broad was sample limited when the spectral slit width was 0.5 nm or less. For the vapor-phase measurements Hg was introduced into 0.100–10.0-cm quartz cells containing air and stoppered securely. The spectral resolution of the atomic resonance transition was limited by the spectral slit width of the spectrometer (0.005–0.015 nm was the lowest attainable with adequate signal to noise ratio) even though the data density was 1500 points/nm. Experimental values of the MCD \bar{A}_1 and \bar{B}_0 parameters and \bar{D}_0 , the electric dipole strength, were determined from a moment analysis¹⁰ of the absorption and MCD spectra as described previously.²

Results and Discussion

Vapor-Phase Spectra. Figure 1 presents the absorption and MCD spectra for Hg vapor in air at room temperature (the vapor pressure of Hg at 24 °C of 1.7×10^{-3} mm corresponds to a molar concentration of 9.2×10^{-8} M) at several magnetic field strengths.

- (1) Jørgensen, C. K. *Absorption Spectra and Chemical Bonding in Complexes*; Addison-Wesley: Reading, MA, 1962; pp 185–189.
- (2) Mason, W. R. *Inorg. Chem.* **1985**, *24*, 2118.
- (3) Sanemasa, I. *Bull. Chem. Soc. Jpn.* **1975**, *48*, 1795 and references cited therein.
- (4) Vinogradov, S. N.; Gunning, H. E. *J. Phys. Chem.* **1964**, *68*, 1962.
- (5) Mitchell, A. G. G.; Zemansky, M. W. *Resonance Radiation and Excited Atoms*; Cambridge University Press: Cambridge, England, 1961.
- (6) Brewer, L.; Meyer, B.; Brabson, G. D. *J. Chem. Phys.* **1965**, *43*, 3973.
- (7) Douglas, I. N.; Grinter, R.; Thomson, A. J. *Mol. Phys.* **1974**, *28*, 1377.

(8) Hatch, W. R.; Ott, W. L. *Anal. Chem.* **1968**, *40*, 2085.

(9) Mason, W. R. *Anal. Chem.* **1982**, *54*, 646.

(10) Piepho, S. B.; Schatz, P. N. *Group Theory in Spectroscopy with Applications to Magnetic Circular Dichroism*; Wiley: New York, 1983.

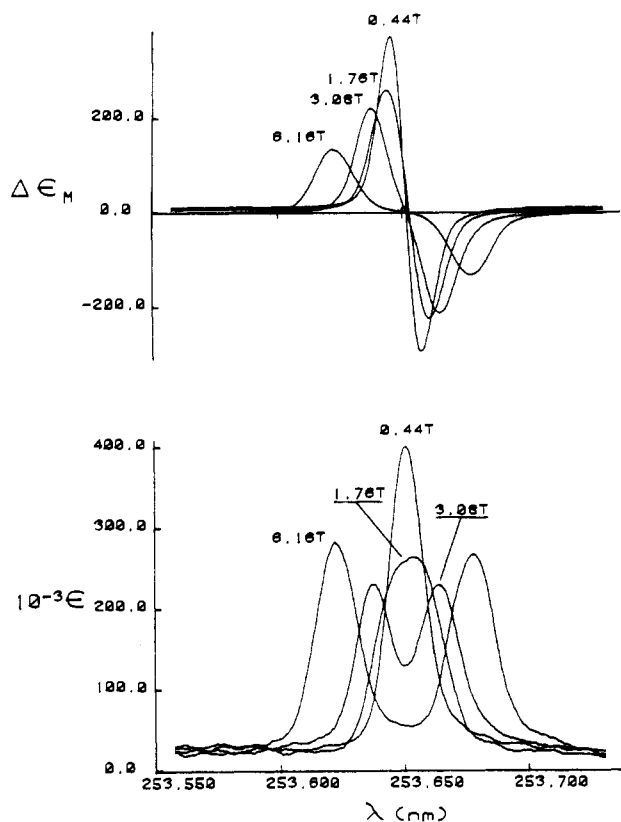


Figure 1. Absorption (lower curves) and MCD (upper curves) spectra for a 10.0-cm path containing Hg vapor (1.7×10^{-3} mm, 24 °C, 9.2×10^{-8} M) in air at different magnetic field strengths. A constant spectral slit width of 0.012 nm was used in each case. $\Delta\epsilon_M$ values were multiplied by 0.001 before plotting and have units of $(\text{M cm T})^{-1}$.

Spectral data are collected in Table I. At low field (0.5 T or less) the absorption spectrum consists of a single line and the MCD shows a very strong positive A term. As the field is increased to 7 T, the single absorption line is clearly resolved into two of nearly equal intensity symmetrically positioned on either side of the zero-field resonance wavelength of 253.65 nm. The MCD A term resolves into a pair of B terms of opposite sign. The positive A term and splitting of the absorption line are due to the Zeeman splitting of the 3P_1 state. When the Zeeman splitting is greater than the line width, as it is here at high field, the resolution of the A term into B terms of opposite sign is a natural consequence of the strong selection rules for the absorption of circularly polarized light by the Zeeman sublevels.¹⁰

Simple theory describes the 3P_1 state, $|A\rangle$, as a combination of 3P_1 and the higher energy 1P_1 state, $|C\rangle$, intermixed by strong Hg spin-orbit coupling ($\zeta 6p = 4260 \text{ cm}^{-1}$).¹ The resonance transition to the $|C\rangle$ state is observed at 184.957 nm.⁵ The two spin-orbit states can be described by eq 1 and 2, where the mixing

$$|A\rangle = -a|^1P_1\rangle + b|^3P_1\rangle \quad (1)$$

$$|C\rangle = b|^1P_1\rangle + a|^3P_1\rangle \quad (2)$$

coefficients $b \geq a$ and $a^2 + b^2 = 1$. From this description of the $|A\rangle$ state, the MCD A term can be characterized by the \bar{A}_1/\bar{D}_0 parameter, which is given by eq 3 for a space-averaged isotropic

$$\bar{A}_1/\bar{D}_0 = (6^{1/2}/3)\langle A||L + 2S||A\rangle \quad (3)$$

sample,^{2,10} where \bar{D}_0 is the dipole strength of the transition and the reduced matrix element contains orbital and spin angular momentum operators. By combining eq 1 and 3, assuming the metal orbitals are pure 6s and 6p Hg atomic orbitals, and evaluating the reduced matrix element, one obtains eq 4. The two

$$\bar{A}_1/\bar{D}_0 = 2|a|^2 + (1 + 2)|b|^2 \quad (4)$$

contributions from the 3P_1 zero-order state (the coefficients of $|b|^2$

Table I. Spectral Data^a

abs		MCD			
λ , nm	$\bar{\nu}$, μm^{-1}	$10^3\epsilon$, $(\text{M cm})^{-1}$	λ , nm	$\bar{\nu}$, μm^{-1}	$10^3\Delta\epsilon_M$, $(\text{M cm T})^{-1}$
Hg Vapor, 0.44 T ^b					
253.6513	3.94242	384	253.6580	3.94232	-310
			253.6525	3.94240	0
			253.6453	3.94251	+390
Hg Vapor, 1.76 T ^b					
253.6533	3.94239		253.6613	3.94226	-227
			253.6536	3.94238	0
			253.6453	3.94251	+273
Hg Vapor, 3.08 T ^b					
253.6660	3.94219	207	253.6660	3.94219	-220
253.6387	3.94262	207	253.6525	3.94240	0
Hg Vapor, 6.16 T ^b					
253.6787	3.94199	236	253.6787	3.94199	-133
253.6227	3.94286	263	253.6507	3.94243	^c
			253.6233	3.94285	+138
Hg in Cyclohexane, 6.16 T ^d					
258.1	3.874	197	258.8	3.864	-0.402
			265.1	3.773	0
254.8	3.925	172	253.7	3.942	+0.584
Hg in Acetonitrile, 6.16 T ^f					
256.1 ^e	3.905	123	257.6	3.882	-0.125
252.0	3.968	134	254.2	3.935	0
			250.5	3.992	+0.181
Hg in Water, 6.16 T ^g					
			258.4	3.870	-0.648
			254.2	3.935	0
			250.0	4.000	+0.636

^a 10.0-cm path; room temperature. ^b $c = 9.2 \times 10^{-8}$ M (vapor pressure at 24 °C = 1.7×10^{-3} mm). ^c Inflection point. ^d $[\text{Hg}] = (5.0 \pm 0.5) \times 10^{-7}$ M; saturated solution. ^e Shoulder. ^f $[\text{Hg}]$ arbitrarily assumed to be 1×10^{-7} M; saturated solution. ^g $[\text{Hg}]$ assumed to be 3.2×10^{-7} (solubility of Hg in water³ at 25 °C); saturated solution.

in eq 4) are due to its orbital and spin angular momentum, respectively. As can be seen from eq 4 the limiting value of \bar{A}_1/\bar{D}_0 for $|A\rangle$ is +3 when $a \sim 0$ and $b \sim 1$ and drops to +2.5 for $a = b = 0.707$ ($|a|^2 = |b|^2 = 0.5$). The value of \bar{A}_1/\bar{D}_0 obtained from moment analyses of spectra at low field (0.1–0.5 T, where the Zeeman splitting is much less than the line width) is $+2.88 \pm 0.19$ with $\bar{\nu}_0 = 3.94242$ (2) μm^{-1} . This result implies $a \sim 0.35$ and $b \sim 0.94$ and, therefore, is consistent with a significant contribution of the singlet zero-order state to $|A\rangle$, which thus provides a rationale for the transition intensity. At higher field the separation of the two absorption lines or the MCD B terms can provide an estimate of the Zeeman splitting, which is given by eq 5, where g is the excited state g factor, μ_B is the Bohr magneton

$$\Delta E = 2g\mu_B H \quad (5)$$

= $0.46680 \text{ cm}^{-1}/\text{T}$, and H is the magnetic field strength. The observed splittings at 3.08 and 6.16 T (see Table I) are 4.2 ± 0.2 and $8.6 \pm 0.2 \text{ cm}^{-1}$, respectively, which are within experimental uncertainty of $\Delta E = 4.25$ and 8.51 cm^{-1} calculated for 3.08 and 6.16 T, respectively, by using eq 5 with $g = 1.479$ from atomic spectral data.¹¹ Furthermore, it can be shown¹⁰ that $\bar{A}_1/\bar{D}_0 = 2g$ and therefore the g value derived from the moment analysis of the MCD at low field is 1.44 ± 0.10 , which is within experimental uncertainty of the value from atomic spectral data.

The very high MCD signal intensity observed for the Hg-vapor measurements (100–300 times larger than normally encountered) deserves comment. This large signal is a result of the narrow atomic absorption line and the strong selection rules for the absorption of left and right circularly polarized light in the transitions to the separate Zeeman sublevels of the $|A\rangle$ state. The MCD is

(11) Moore, C. E. *Natl. Bur. Stand. Circ. (U.S.)* 1958, No. 467, vol. III.

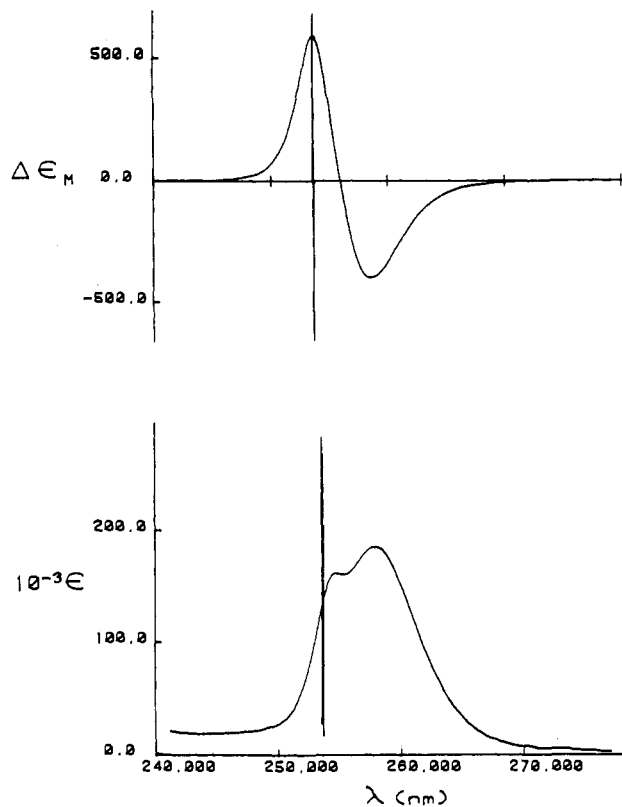


Figure 2. Absorption (lower curve) and MCD (upper curve) spectra for 5.0×10^{-7} M Hg in cyclohexane (saturated) measured at 6.16 T for a 10.0-cm path. Plotted for comparison are the 6.16-T vapor-phase spectra (Figure 1; the $\Delta\epsilon_M$ values multiplied by 0.005 before plotting).

a difference absorption measurement between left and right circularly polarized light, $\Delta A = A_l - A_r$. As the transitions to the Zeeman sublevels separate in energy in the presence of the field, ΔA for each transition becomes large because A_r (or A_l) becomes small, and eventually when separate transitions are resolved, $\Delta A \approx A_l$ (or $\Delta A = -A_r$) and thus approaches the magnitude of half the total absorbance $A = A_l + A_r$ in the ideal case where $A_l = A_r$. Within acceptable signal to noise considerations for ΔA , the sensitivity of the measurements using a modern CD spectrometer is $\sim 10^{-4}$ – 10^{-5} optical density unit, which may be compared to 10^{-2} – 10^{-3} for absorbance measurements using a conventional spectrophotometer. Thus MCD, even at modest field strengths, offers an improvement of 10–100 times in the sensitivity for Hg-vapor detection over absorbance under the same conditions of path length and vapor concentration and, therefore may have utility for trace Hg detection and analysis.

Solution Spectra. Figure 2 presents absorption and MCD spectra for saturated solutions of Hg in cyclohexane, while Figure 3 shows the spectra for saturated solutions in water or acetonitrile. In each case the derivative-shaped A term is observed in the MCD spectra. The signal to noise ratio is most favorable for the cyclohexane solution, and Beer's law was verified for a 10-fold dilution. The aqueous measurement was quite weak, and as Figure 3, shows the absorption band is virtually obscured by background. The broadness of the solution spectra is emphasized by comparison with the Hg-vapor spectra, which are also plotted in Figures 2 and 3. The splitting of the absorption band described earlier is clearly seen in the cyclohexane and acetonitrile absorption spectra. This splitting is accompanied by a noticeable unsymmetrical shape for the A term—the long-wavelength negative portion is broader than the short-wavelength positive portion.

The cyclohexane spectra are of sufficient quality that a reliable moment analysis for both absorption and MCD could be obtained over the entire band system. The results gave a value for \bar{A}_1/\bar{D}_0 of $+2.7 \pm 0.1$ with $\bar{\nu}_0 = 3.883$ ($1 \mu\text{m}^{-1}$). This value of \bar{A}_1/\bar{D}_0 is not significantly different from the vapor-phase value reported above; however, $\bar{\nu}_0$ here is the average energy of the two absorption

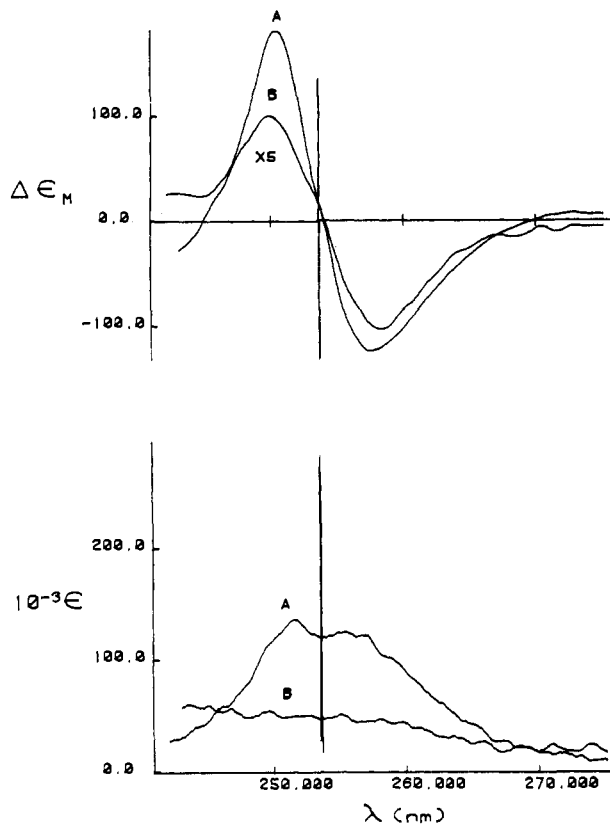


Figure 3. Absorption (lower curves) and MCD (upper curves) spectra for saturated solutions of Hg in acetonitrile (A) and water (B) at 6.16 T for a 10.0-cm path. The concentration for the acetonitrile spectra was arbitrarily chosen to be 1×10^{-7} M while that for water was taken to be 3.2×10^{-7} M from ref 3. The MCD in water was multiplied by a factor of 5 before plotting. Plotted also for comparison are the 6.16-T vapor-phase spectra (Figure 1; the $\Delta\epsilon_M$ values multiplied by 0.001 before plotting).

components and therefore differs from the vapor-phase result. In the earlier study of Bi(III), Pb(II), and Tl(I) in aqueous acid solution² the broad A terms gave values of \bar{A}_1/\bar{D}_0 in the range $+1.9$ to $+2.1$ and it was argued that values lower than $+2.5$ to $+3$ implied quenching of orbital angular momentum. The most reasonable explanation for quenching was suggested as participation of the 6p orbitals in covalent bonding to H_2O molecules in aqueous solutions. In the present case the similarity of the gas and solution values of \bar{A}_1/\bar{D}_0 , together with the small ratio of a/b from eq 4, implies only a minimal angular momentum quenching and therefore only weak participation of the Hg 6p orbitals in covalent bonding to cyclohexane solvent molecules. This conclusion is reasonable when the "noble" character of Hg and the weakness of cyclohexane as a potential ligand are considered.

The question remains as to the origin of the band broadening and splitting. Several suggestions were considered earlier.⁴ Among those considered less likely was a shift of either the 3P_2 or 3P_0 state closer in energy to 3P_1 (resonance transitions $^1S_0 \rightarrow ^3P_2$ and $^1S_0 \rightarrow ^3P_0$ have been observed at 227.0 and 265.6 nm, respectively,¹¹ in the vapor phase but both are very weak). Both of these states are forbidden and transitions to them in solution are expected to be weak. The MCD for the nondegenerate 3P_0 should be especially weak since only second-order effects could provide B term intensity. Further, a large solvent shift of either of these forbidden states would be difficult to justify with only a minimal shift of the 3P_1 state (the broad absorptions in solution are still centered near the vapor-phase resonance energy). Also considered unlikely was the possibility of two (or more) different solvent cavities for the Hg atoms. This possibility would predict two symmetrical A terms rather than one unsymmetrical envelope. The suggestion considered most reasonable, and one that is compatible with the present results is that the excited state in solution is distorted (Jahn-Teller distortion) from the totally symmetric ground state.

If the distortion were either tetragonal or trigonal, for example, the 3-fold degeneracy of the A_1 state would be lifted and a pair of states of A_2 and E symmetries would result. The present results cannot distinguish between these two types of distortion in any easy way, but simple considerations in both cases lead to the prediction of a positive A term for the degenerate E state and B terms of opposite sign for the A_2 and E states, respectively, which would give rise to a positive pseudo A term if the two states are close in energy (within bandwidths). The combination of the A term for the E state and the pseudo A term for the interaction between the A_2 and E states would be expected to give an unsymmetrical MCD spectrum as observed. The A_2 state is likely lower in energy than the E state and has the negative B term because the reverse possibility would tend to make the positive short-wavelength part of the MCD spectrum broad and the long-wavelength part narrow. In view of the broadness of the spectra a more extensive or detailed analysis of the cyclohexane spectra is not possible.¹⁵ However it is worthwhile to note that Mg atoms isolated in noble-gas matrices reveal similar MCD and absorption features with more detail for the $^1S_0(3s^2) \rightarrow ^1P_1(3s3p)$ transition.¹² A moment analysis of MCD and absorption as-

suming an octahedral environment showed a dominant contribution to the bandwidth from noncubic (Jahn-Teller-active) modes. Similar conclusions were reached from detailed analyses of absorption and MCD spectra for Li and Na atoms in noble-gas matrices, where the transitions $^2S(rs^1) \rightarrow ^2p(mp^1)$ were studied.^{13,14} A careful analysis of the MCD for matrix-isolated Hg is a logical extension of this work and is planned in the future.

Acknowledgment. Helpful discussions with Dr. C. T. Lin are gratefully acknowledged.

Registry No. Hg, 7439-97-6; NCMe, 75-05-8; H₂O, 7732-18-5; cyclohexane, 110-82-7.

- (12) Mowery, R. L.; Miller, J. C.; Krausz, E. R.; Schatz, P. N.; Jacobs, S. M.; Andrews, L. *J. Chem. Phys.* **1979**, *70*, 3920.
- (13) Lund, P. A.; Smith, D.; Jacobs, S. M.; Schatz, P. N. *J. Phys. Chem.* **1984**, *88*, 31.
- (14) Rose, J.; Smith, D.; Williamson, B. E.; Schatz, P. N.; O'Brien, M. C. *M. J. Phys. Chem.* **1986**, *90*, 2608.
- (15) A reviewer has offered an alternative suggestion that the unsymmetrical shape of the solution spectra may arise from transitions to a distorted potential surface that is due to vibronic coupling of the solvent cage modes with the Hg atom excited state.

Contribution from the Lehrstuhl für Anorganische Chemie I der Ruhr-Universität, D-4630 Bochum, FRG, Institut für Anorganische Chemie der Johann-Wolfgang-Goethe-Universität, D-6000 Frankfurt/Main, FRG, and Max-Planck-Institut für Strahlenchemie, D-4330 Mülheim an der Ruhr, FRG

Redox Reactivity of Bis(1,4,7-triazacyclononane)iron(II/III) Complexes in Alkaline Solution and Characterization of a Deprotonated Species: Amidoiron(III) vs Aminyliron(II) Ground-State Formulation. EPR, Kinetic, Pulse Radiolysis, and Laser Photolysis Study

Klaus Pohl,^{1a} Karl Wieghardt,^{*1a} Wolfgang Kaim,^{1b} and Steen Steenken^{1c}

Received July 30, 1987

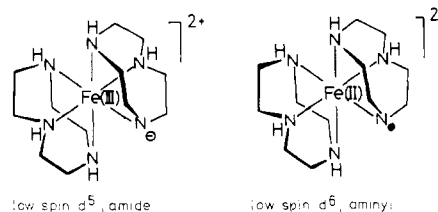
The redox reactivity of the low-spin complexes $[\text{FeL}_2]^{3+}$ and $[\text{FeL}_2]^{2+}$ ($L = 1,4,7\text{-triazacyclononane}, C_6H_{15}N_3$) in alkaline aqueous solution has been investigated. Orange $[\text{Fe}^{\text{III}}\text{L}_2]^{3+}$ is reversibly deprotonated ($pK_a = 11.4 \pm 0.4$) in alkaline solution to yield a deep blue species ($\lambda_{\text{max}} = 542 \text{ nm}$; $\epsilon = 1.8 \times 10^3 \text{ M}^{-1} \text{ cm}^{-1}$), which has been characterized by its frozen-solution EPR spectrum as the low-spin amidoiron(III) complex, $[\text{Fe}^{\text{III}}\text{L}(\text{L-H})]^{2+}$ ((L-H) is the N-deprotonated form of the ligand L). The aminyl radical iron(II) formulation, $[\text{Fe}^{\text{II}}\text{L}(\text{L-H})]^{2+}$, is proposed to be an electronically excited state (ligand-to-metal charge transfer). $[\text{Fe}^{\text{III}}\text{L}(\text{L-H})]^{2+}$ disproportionates slowly under anaerobic conditions to yield 50% $[\text{Fe}^{\text{II}}\text{L}_2]^{2+}$ and probably 50% $[\text{LFe}^{\text{II}}(\text{OH}_2)_3]^{2+}$ and a two-electron-oxidation product of one 1,4,7-triazacyclononane ligand, which has not been characterized. In the presence of an external oxidant (H_2O_2 or oxygen) the blue species decomposes to produce quantitatively 1 equiv of oxidized macrocycle and $[\text{Fe}^{\text{III}}\text{L}(\text{OH}_2)_3]^{3+}$. The kinetics of both reactions have been measured. Pulse radiolysis experiments have shown that the oxidation of $[\text{FeL}_2]^{2+}$ with Br_2^- , I_2^- , and $(\text{SCN})_2^-$ and oxygen-centered radicals such as OH^\bullet and the phenoxyl radical yield $[\text{Fe}^{\text{III}}\text{L}_2]^{3+}$ at nearly diffusion controlled rates in the pH range 4–10. At higher pH values (11–13) the blue amidoiron(III) species is formed. $[\text{Fe}^{\text{III}}\text{L}(\text{L-H})]^{2+}$ oxidizes ascorbate(2-) to give $[\text{Fe}^{\text{II}}\text{L}_2]^{2+}$ and the ascorbate(1-) radical. Laser photolysis of solutions of $[\text{FeL}_2]^{2+}$ at pH 8–10 with 20-ns pulses from a KrF excimer laser ($\lambda = 248 \text{ nm}$) produces $[\text{FeL}_2]^{3+}$ and the hydrated electron with a quantum yield of 0.9; at pH > 10 $[\text{FeL}(\text{L-H})]^{2+}$ and $e^-(\text{aq})$ are produced at the same rate.

Introduction

We have recently reported the synthesis and spectroscopic properties of two low-spin iron(III) and iron(II) complexes, each of them containing two molecules of the cyclic tridentate ligand 1,4,7-triazacyclononane (L).² These were examples of low-spin iron(II/III) complexes in an octahedral environment of six saturated amine nitrogen atoms. The structures of $[\text{FeL}_2]\text{Cl}_2 \cdot 4\text{H}_2\text{O}$ and $[\text{FeL}_2]\text{Cl}_3 \cdot 5\text{H}_2\text{O}$ were subsequently determined by X-ray crystallography.³ $[\text{FeL}_2]^{2+}$ is remarkably stable in aqueous solution in the pH range 6–13. No ligand dissociation has been observed at 25 °C for 6 h. The same was found to be true for orange $[\text{FeL}_2]^{3+}$ in the pH range 2–10, but at pH > 10 a dramatic color change of such solutions to deep blue is observed. This color

change is completely reversible; reacidification restores quantitatively the $[\text{FeL}_2]^{3+}$ species.

In this paper we describe the nature of this blue species and the redox properties of $[\text{FeL}_2]^{3+}$ and $[\text{FeL}_2]^{2+}$. As we will show, the blue species is the monodeprotonated form of $[\text{FeL}_2]^{3+}$; we will abbreviate the N-deprotonated form of the parent ligand 1,4,7-triazacyclononane as (L-H) , $(C_6H_{14}N_3)^-$. One of the questions to be answered is the problem of the electronic ground state of this blue species; i.e., are we dealing with an amidoiron(III) or, alternatively, an aminyliron(II) radical dication?



Species like this have been postulated as reactive intermediates

- (1) (a) Ruhr-Universität Bochum. (b) Universität Frankfurt. (c) Max-Planck-Institut Mülheim an der Ruhr.
- (2) Wieghardt, K.; Schmidt, W.; Herrmann, W.; Küppers, H. *J. Inorg. Chem.* **1983**, *22*, 2953.
- (3) Boeyens, J. C. A.; Forbes, A. G. S.; Hancock, R. D.; Wieghardt, K. *Inorg. Chem.* **1985**, *24*, 2926.